Article

Customized Utilization Strategies of Industrial Lignin to Produce Adsorbents and Flocculants Based on Fractionation and Adequate Structural Interpretation

Lei Wang [1],*, Dewei Yang [1], Xiaohan Li [1], Xinyi Zhu [1], Jungang Jiang [1], Yifan Zhang [1], Xue Chen [2] and Hongbo Yu [3]

[1] Hubei Provincial Key Laboratory of Green Materials for Light Industry, School of Materials and Chemical Engineering, Hubei University of Technology, Wuhan 430068, China; y13235634365@163.com (D.Y.); lxiaohan0317@163.com (X.L.); 102000414@hbut.edu.cn (X.Z.); jungang.jiang@hbut.edu.cn (J.J.); zhangyifan@hbut.edu.cn (Y.Z.)

[2] School of Engineering, Jining University, Qufu 273155, China; chenxue37121@163.com

[3] Key Laboratory of Molecular Biophysics of MOE, College of Life Science and Technology, Huazhong University of Science and Technology, Wuhan 430074, China; yuhongbo@hust.edu.cn

* Correspondence: wanglei@hbut.edu.cn

Abstract: Lignin, a by-product of pulping and biorefinery, has great potential to replace petrochemical resources for wastewater purification. However, the defects of lignin, such as severe heterogeneity, inferior reactivity and poor solubility, characterize the production process of lignin-based products by high energy consumption and serious pollution. In this study, several lignin fractions with relatively homogeneous structure were first obtained by organic solvent fractionation, and their structures were fully deciphered by various characterization techniques. Subsequently, each lignin component was custom-valued for wastewater purification based on their structural characteristics. Benefiting from the high reactivity and reaction accessibility, the lignin fraction (lignin-1) refined by dissolving in ethanol and n-butanol could been used as a raw material to produce cationic lignin-based flocculant (LBF) in a copolymerization system using green, cheap and recyclable ethanol as solvent. The lignin fraction (lignin-2) extracted by methanol and dioxane showed low reactivity and high carbon content, which was used to produce lignin-based activated carbon (LAC) with phosphoric acid as activator. Moreover, the influences of synthetic factors on the purification capacity were discussed, and the LBF and LAC produced under the optimal conditions showed distinguished purification effect on kaolin suspension and heavy metal wastewater, respectively. Furthermore, the corresponding purification mechanism and external factors were also elaborated. It is believed that this cleaner production strategy is helpful for the valorization of lignin in wastewater resources.

Keywords: fractionation; lignin-based flocculants; lignin-based activated carbons; purification mechanism; wastewater resources

1. Introduction

The improvement of living quality and the rapid development of industrial technologies are making the composition of actual wastewater increasingly complex, coupled with the rapid growth of the population, resulting in a serious water crisis [1]. Wastewater recycling is an effective way to solve the water crisis [2]. Flocculation and adsorption are indispensable steps to purify wastewater, and the development of efficient, green and sustainable flocculants and adsorbents is crucial [3]. Considering the increasingly serious environmental problems and the depletion of petrochemical resources, it is urgent to develop natural polymer-based materials featuring high efficiency, low cost, raw material regeneration, and no secondary pollution for wastewater recycling.

Lignin, the most abundant renewable aromatic resource, is a high-volume by-product arising from pulping and biorefinery [4]. Lignin has a high amount of reactive functional

groups (e.g., -OH, -COOH, and -OCH$_3$), a rigid core skeleton and high carbon content, which give it great potential to produce flocculants and adsorbents [5,6]. Research on the application of lignin in flocculants [7], adsorbents [8], hydrogels [9], composites [10], and thermoplastics [11] has been carried out for a long time. However, great breakthroughs have not been made in the industrial process of lignin-based materials in spite of large quantities of studies, which is mainly due to the severe heterogeneity of lignin caused by plant species, biosynthesis and extraction processes [12,13].

Reducing the heterogeneity of lignin and customizing the utilization according to the structural characteristics of each component are effective strategies to overcome the aforementioned problems. To make lignin more uniform, several fractionation methods have been developed [14]. However, the pH acidic precipitation method, membrane separation method and gel permeation chromatography method have the disadvantages of low efficiency [15], high cost due to a high amount of filter membranes [16], and complex equipment [17], respectively. The organic solvent fractionation has the advantages of easy operation, low costs, and recoverable solvents [18]. Several lignin fractions with homogeneous structures can be obtained by organic solvent fractionation in accordance with physicochemical properties [19,20]. Moreover, after fully deciphering the structure of each lignin component, they can be custom applied according to their structural characteristics, which greatly promotes the development of lignin-based products. Lignin refined by sequential solvent fractionation has been successfully used for the production of lignin-based epoxy resins owing to its relatively low dispersion [12]. Unfortunately, only part of the fractionated lignin fraction was used in these studies, and there are no reports on the utilization of the remaining lignin fraction. Furthermore, there is little research on the utilization of fractionated lignin in wastewater resources.

In order to solve the problems of poor reactivity and solubility of lignin, dioxane, dimethyl sulfoxide and high-concentration alkali liquor are usually used as reaction solvents in the production of lignin-based flocculants [21,22]. These reaction solvents can cause serious environmental burden and high cost [23]. Ethanol as a reaction solvent has excellent application prospects due to its low price, non-toxicity, and easy recovery [24]. However, most industrial lignin is only partially soluble in ethanol, limiting the application of ethanol as a solvent to produce lignin-based flocculants [25]. Therefore, refining to obtain lignin components that can be completely dissolved in ethanol and have high reactivity is a practical idea for realizing the green synthesis of lignin-based flocculants in ethanol solution. Note that the lignin components remaining after refining with the above requirements usually have large molecular weight and high carbon content, which are suitable as precursors for the production of lignin-based activated carbons.

In this study, industrial alkali lignin was first divided into several more homogeneous lignin components by organic solvent fractionation, and their structures were adequately deciphered. Subsequently, according to the structural characteristics, fractionated lignin components have been used as raw materials to produce different materials for purifying wastewater. The lignin-based flocculant was produced in the copolymerization system where a lignin component with superior solubility and reactivity was used as raw material, trimethyl-2-methacroyloxyethylammonium chloride as the monomer, and ethanol as the solvent, and the kaolin suspension was employed to test its flocculation performance. Lignin-based activated carbon was produced using lignin components with larger molecular weight and higher carbon content as precursors for the adsorption of heavy metals in wastewater. Moreover, the purification mechanisms of lignin-based flocculant and lignin-based activated carbon in the purification of wastewater were systematically explored. Furthermore, the influences of external factors on the purification effects were discussed in detail.

2. Results and Discussion

2.1. Classification of Lignin and the Characterization of its Components

Considering the effects of binding energy and hydrogen bonding capacity for lignin-dissolving properties in organic solvents, four organic solvents including n-butanol, ethanol, methanol, and dioxane were selected. As shown in Table 1, the yields of F1-F5 were 15%, 34.93%, 19.10%, 21.22%, and 9.15%, respectively. Before fractionation, KL showed a molecular weight (2777 g/mol) with a PDI up to 3.15. The fractionated lignin components (F1-F4) were more homogeneous, and their Mw increased sequentially, at 1141, 2696, 3987, 6794, and 9820 g/mol, respectively. Notably, the phenolic hydroxyl content of lignin decreased as its molecular weight increased, which was because the cleavage of the ether bond produced more phenolic hydroxyl groups. F1 and F2 had higher phenolic hydroxyl content than KL, which were more suitable to produce lignin-based products by free radical polymerization.

Table 1. Yields and structure information of lignin samples.

Lignin Samples	Yield (%)	Mn (g/mol)	Mw (g/mol)	PDI	Total Phenolic$-$OH (mmol/g)	COOH (mmol/g)
KL		881	2777	3.15	4.53	2.72
F1	15.00	781	1141	1.46	4.97	3.12
F2	34.93	1885	2696	1.43	4.55	2.74
F3	19.10	2807	3987	1.42	3.17	1.56
F4	21.22	4355	6794	1.56	2.77	1.26
F5	9.15	4676	9820	2.10	2.30	1.21

Structural information for all samples obtained by FT-IR is shown in Figure S1. The main signals appear at 1598, 1508, and 1420 cm^{-1} (aromatic skeletal vibrations), which indicated that the lignin retains its typical structure [26]. However, lignin with higher molecular weight had lower relative strength of unconjugated carbonyl stretching at 1712 cm^{-1} [26]. This phenomenon revealed that the carboxyl groups in lignin with a decrease were favored by a higher molecular weight, which was consistent with that of ^{31}P NMR.

Figures 1 and S2 show the 2D-HSQC NMR spectra of all lignin samples, and the corresponding cross-signals refer to previous studies [27–29]. In terms of the side chain region, it could be observed that β-*O*-4 was the main linkage between the lignin units. The lignin component with a stronger β-*O*-4 signal displayed a larger molecular weight, which was consistent with the results of previous studies [30]. Moreover, the cleavage of the β-*O*-4 linkage might generate phenolic hydroxyl groups, therefore the lignin component with a small molecular weight showed a higher content of phenolic hydroxyl groups [31]. In addition, no cross-linking signals related to carbohydrates were observed in all lignin samples, indicating that these lignin samples were pure and had good application prospects. For the aromatic region, in addition to the cross-linking signals attributed to S, G, and H units, a distinct signal for dissociative *p*-coumaric acid (*p*-CA) was also observed, showing a typical lignin structure isolated from corn cob. It was found that the proportion of lignin-containing S units with an increase is favored by a higher molecular weight. Considering the active site and steric hindrance, the lignin consisting of low molecular weight had relatively more H and G units and exhibited higher reactivity.

Combined with the above analysis, F1 and F2 with lower molecular weight showed more Ph-OH groups. Therefore, lignin-1 (F1 and F2) used as a raw material showed noticeable benefits for the production of lignin-based flocculant. The lignin-2 (F3 and F4) had higher molecular weight and fewer phenolic hydroxyl (Ph-OH) and carboxyl groups (-COOH), resulting from higher carbon content. They were suitable as precursors for the production of lignin-based activated carbon. F5 accounted for a small proportion and contained a large number of impurities, so it was not included in the follow-up study.
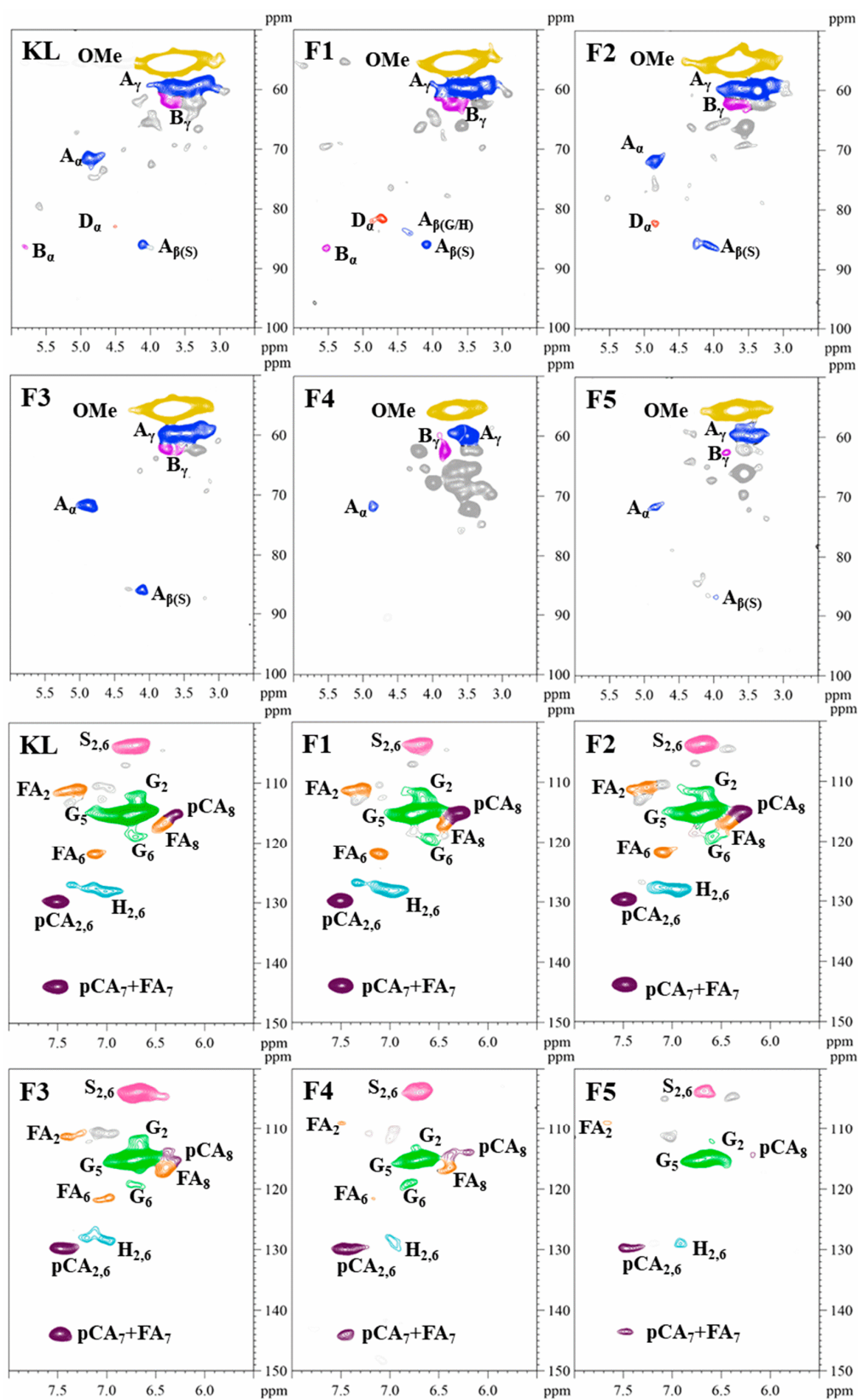
Figure 1. The side chain region (δ_C/δ_H 50–100/2.5–6.0) and aromatic region (δ_C/δ_H 100–150/5.5–8.0) in the 2D HSQC NMR spectra of lignin samples. The alkali lignin (KL) isolated from corn cob, the lignin fractions collected from n-butanol, ethanol, methanol, and dioxane were referred as F1, F2, F3, and F4, respectively, and F5 was an insoluble residue.

2.2. Production of Lignin-Based Flocculant

The polymerization mechanism is shown in Scheme S1. First, AIBN was decomposed to produce primary free radicals at high temperature. The phenolic hydroxyl group of lignin was attacked by primary free radicals, producing phenolic oxygen radicals. Meanwhile, these primary radicals attacked the alkenyl groups of METAC and produced METAC radicals, finally obtaining a lignin-based flocculant [32,33]. In addition, the PMETAC was produced as a side effect by polymerization between METAC radicals (as shown in Scheme S1B).

The flocculation property of lignin-based flocculant is determined by a variety of internal factors, for example hydrophilicity, charge density, and molecular weight, which are determined by the production conditions [34]. Therefore, production conditions such as the dosage ratio of MEATC and lignin, reaction time and reaction temperature were performed in this study. The synthesis process and structural information of lignin-based flocculants were recorded in Table S1.

The ratio of MEATC to lignin shows an effect on the flocculation performance of lignin-based flocculant (Figure 2A). As the METAC dosage increased, the removal of kaolin suspension by lignin-based flocculant first increased and then decreased. This was because more METAC monomer could increase the grafting rate of lignin, so that more METAC was grafted onto the lignin backbone. Therefore, the lignin-based flocculant produced under the larger METAC dosage ratio had higher molecular weight and positive charge density, exhibiting better flocculation performance. However, an excess of METAC monomers would cause a large number of homo-polymerization reactions, thereby reducing the grafting rate and flocculation property of lignin-based flocculant [33]. The effect of reaction time on flocculation ability of lignin-based flocculant is shown in Figure 2B. The flocculation property of lignin-based flocculant improved rapidly as reaction time increased (from 2 h to 4 h). A longer time was helpful for the sufficient progress of the copolymerization of lignin and METAC. However, the flocculation property of lignin-based flocculant hardly changed when the reaction time exceeded 4 h. Furthermore, the flocculation property of lignin-based flocculant affected through change in reaction time was also investigated (Figure 2C). The degree of substitution of lignin increased as temperature increased at the initial stage, and the flocculation ability of lignin-based flocculant was improved. This phenomenon suggested that the polymerization reaction was an endothermic reaction, namely that the higher temperature facilitated the excitation of free radicals and the polymerization between free radicals, yet at the same time the chain transfer reaction and chain termination reaction hindered the copolymerization of lignin and METAC at high temperature over 60 °C [35]. Regarding the above discussion, the optimum production conditions of lignin-based flocculant (LBF) for flocculating kaolin were as follows: ratio of MEATC and lignin of 4, reaction time of 4 h and reaction temperature of 60 °C. The production of LBF was performed using the above conditions as the object of subsequent research.
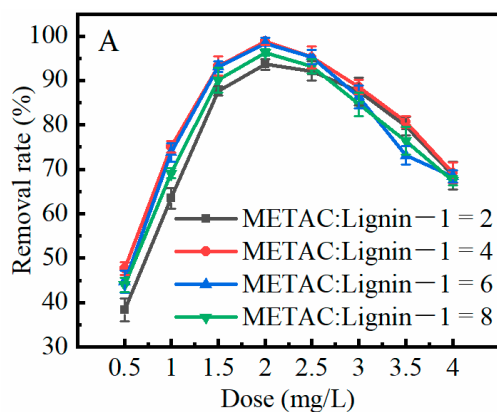

Figure 2. *Cont.*
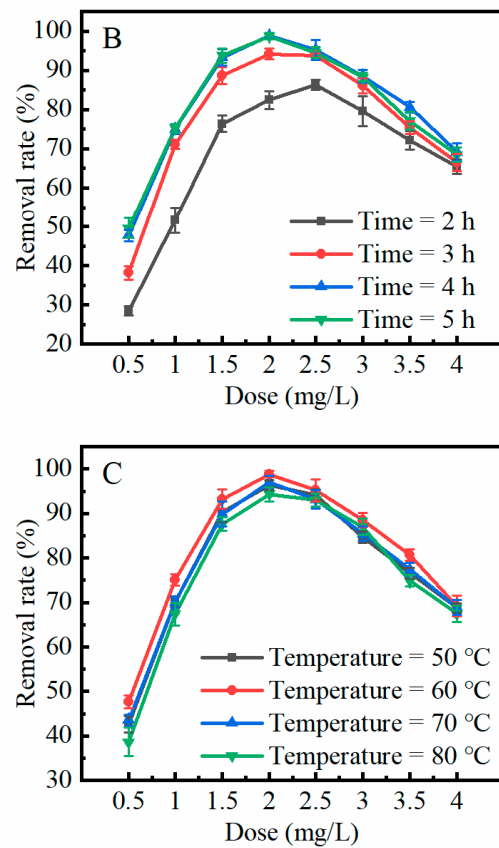
Figure 2. Effect of production conditions on removal rate of lignin-based flocculant: (**A**) impregnation ratio, (**B**) time, and (**C**) temperature. Error bars represent the standard deviation from three repetitions.

2.3. Characterization of Lignin-Based Flocculant

The FT-IR spectra of lignin-1, LBF, and PMETAC are shown in Figure 3A. The signals detected at 1604, 1511 and 1428 cm^{-1} on lignin-1 and LBF are attributed to the characteristic peak of lignin aromatic skeleton, and new peaks for LBF that occurred at 1726, 1480, and 953 cm^{-1} are primary derived from the C=O, C-N, and -OCH$_3$ of quaternary ammonium, respectively [26,36,37]. These characteristic signals were agreed with the assignment of PMETAC FT-IR bands, which preliminarily proved that PMETAC can be grafted into the skeleton of lignin. Moreover, the signal intensity attributed to the phenolic hydroxyl group in lignin was weakened at 1033 cm^{-1}, confirming that the copolymerization took place on the phenolic hydroxyl group of lignin [37].
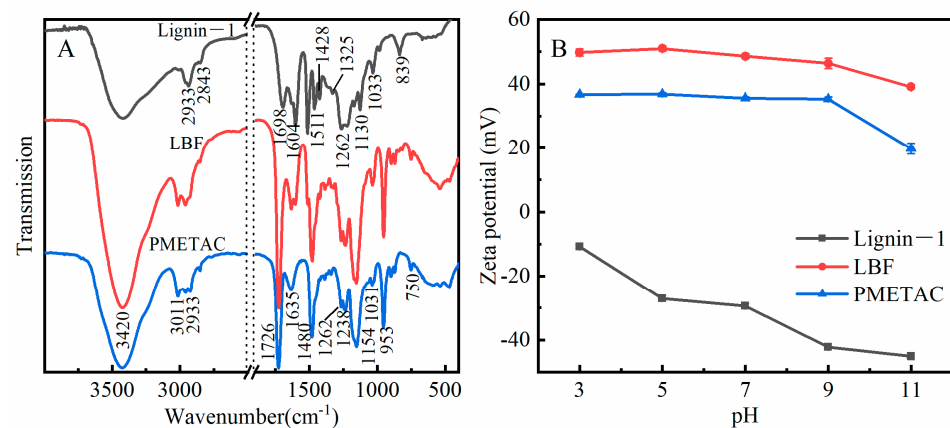

Figure 3. (**A**) FTIR spectra of Lignin-1, PMETAC and LBF, (**B**) zeta potential of Lignin-1, PMETAC and LBF as function of the pH.

Figure 3B compares the zeta potentials of lignin-1, LBF, and PMETAC at different pH values [38]. The measurements showed that the zeta potentials of lignin-1 in solutions with pH values between 3 and 11 were negative because of the negatively charged groups (carboxyl group and phenolic hydroxyl groups). However, after copolymerization, the cationic group of METAC was grafted to lignin. Therefore, the LBF exhibited a higher positive charge density, and showed positive zeta potentials over all pH ranges. It was worth noting that the lignin skeleton provided a rigid core for LBF, which enabled LBF to have a more stable form in water. Therefore, the LBF has a higher positive charge density than PMETAC, which proved further that METAC had been successfully grafted into the skeleton of lignin.

2.4. External Factors Influencing the Flocculation Effect

Investigating the effect of external factors on the flocculation efficiency can evaluate the commercial prospects of LBF. Figure 4A shows the effect of the LBF dosage on the removal rate of the kaolin suspension and the zeta potential of the corresponding supernatant. The removal rate of kaolin suspension went up first with increases in LBF dosage and then decreased, and the best turbidity removal rate of LBF for kaolin suspension was 98.87% at 2 mg/L dosage. In the initial increasing stage of LBF dosage, since the kaolin suspension contains a number of negative charges, the addition of more LBF with positive charges could destabilize the kaolin particles under the action of electrostatic attraction, thereby promoting the flocculation effect. At this time, a number of negative charges in the kaolin suspension were rapidly neutralized, so the zeta potential increased rapidly. Until optimal flocculation was achieved, the potential of the supernatant approached zero, which was consistent with the classical charge neutralization theory [39]. As the dosage of LBF continued to increase, the increase of the zeta potential resulted in lower removal rate. This was because LBF increased the electrostatic repulsion between particles, resulting in a re-stabilization phenomenon.

Figure 4B shows the effect of the initial kaolin concentration (C_0) on the removal rate, and LBF showed significant flocculation effects at all four different initial concentrations of kaolin suspension. As the C_0 increased, the total amount of negative charge also increased, therefore a larger dosage of LBF was required. However, the optimal dosage was far lower than the theoretical calculated value, which was a typical flocculation system dominated by bridging [40–42].

The effect of kaolin suspension pH on the removal rate is shown in Figure 4C. When the suspension pH was in the range of 4 to 8, the removal rate of LBF to the kaolin suspension was higher than 95% at the dosage of 2 mg/L, which showed a satisfactory adaptability to the wastewater pH. Under acidic conditions, the flocculation effect of LBF was slightly enhanced due to protonation. When wastewater pH was 10, LBF eliminated 90% of kaolin suspension at the optimal dosages of 2.5 mg/L. This was because many hydroxide ions reduced the electrostatic attraction of LBF through deprotonation, thereby reducing the flocculation ability of LBF [43].

The influences of coexisting ions Ca^{2+} and SO_4^{2-} on the flocculation efficiencies of LBA were studied (Figure 4D). The results showed that the flocculation effect of LBF was slightly improved by adding a high concentration of Ca^{2+}. The presence of Ca^{2+} could strengthen the electrostatic attraction between LBF and kaolin particles, thereby promoting the formation of flocs and increasing the flocculation effect. Conversely, the presence of SO_4^{2-} weakened the electrostatic attraction, reduced the flocculation effect and increased the consumption of LBF. However, LBF exhibited outstanding flocculation effect whether it was faced with wastewater with high concentration of anions or cations. In general, LBF could be applied to various complex external factors, such as wastewater with different initial concentrations, a wide range of pH and coexisting ions.
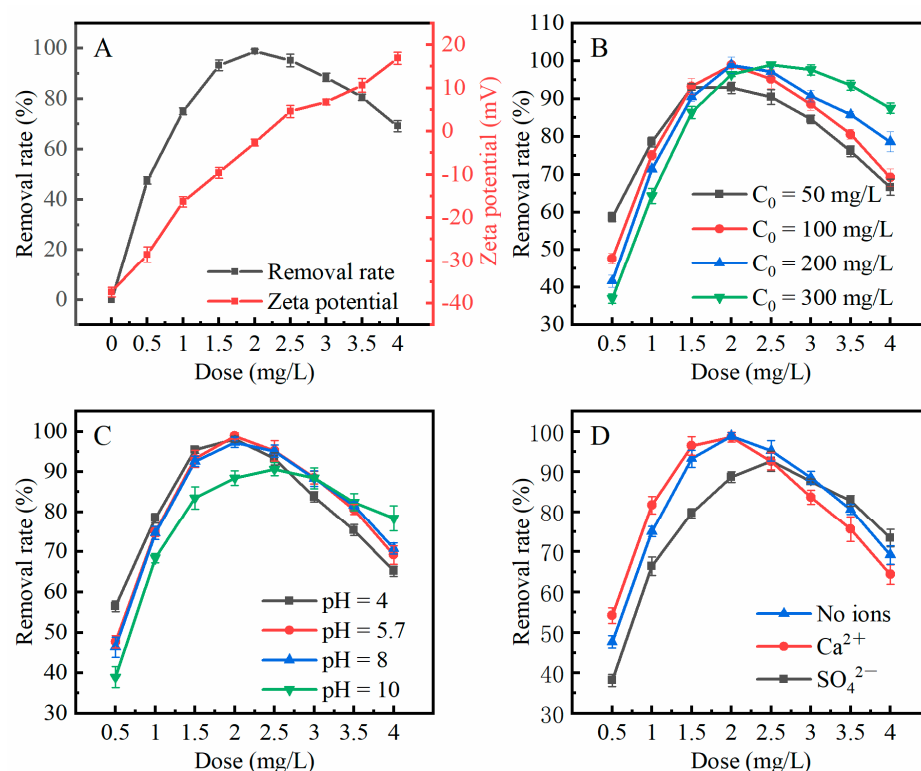
Figure 4. Effects of (**A**) dose, (**B**) initial concentration of the kaolin suspension, (**C**) suspension pH and (**D**) coexisting ions on the removal rate. Error bars represent the standard deviation from three repetitions.

Scheme 1 shows the flocculation mechanism of LBF on the kaolin suspension. The kaolin particle surface was negatively charged, and the LBF had positive charge, so the flocculation process in the kaolin suspension treatment was mainly charge attraction, and then the flocculation group was formed through bridging [32,42].
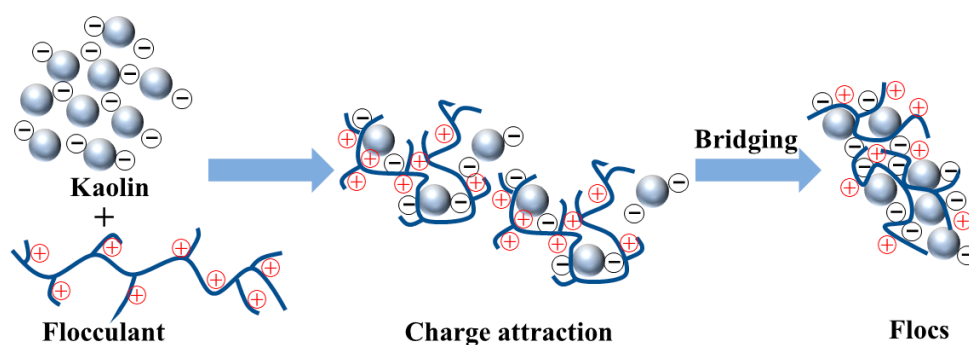
Scheme 1. Flocculation mechanism of lignin-based flocculant on kaolin suspension.

2.5. Production and Characterization of the Lignin-Based Activated Carbon

Table S2 shows the BET of lignin-based activated carbon produced under different impregnation ratios of phosphoric acid to lignin, which showed that the BET increased with the increase in impregnation ratio. The lignin-based activated carbon produced with the impregnation ratio of 2.5:1 had the largest BET of 806.74 m^2/g, which was used as the follow-up research object and named LAC.

The structures of lignin-2 and LAC were revealed by FT-IR, XPS and SEM (see Figure 5). As shown in the FT-IR spectra (Figure 5A), the main signals appear at 1603, 1512 cm^{-1} (aromatic skeletal vibrations), and the absorption peak at 1460 cm^{-1} is attributed to the C-H deformation in –OCH$_3$. The bands at 1122 and 871 cm^{-1} were prominent, indicating

the presence of C-O and C=O [26]. Compared with lignin, the characteristic peak signals and intensities of LAC spectrum were significantly reduced, indicating that bonding bonds and functional groups on the lignin were largely destroyed during the high-temperature activation. However, some signals of oxygen-containing functional groups could still be observed, which contributed to the adsorption of heavy metal ions through chelation.

XPS results are shown in Figure 5B–D. Figure 5B shows that both lignin-2 and LAC had high C, O elements and few N elements, while LAC contained few P elements due to phosphoric acid activation. LAC had lower O element and higher C element than F4, which was attributed to the high-temperature activation. Moreover, for Figure 5C,D, the signals of lignin-2 XPS spectra at 533.95 eV, 533.00 eV, and 531.58 eV were caused by C-OH, -O-, C=O, and their contents are 10.24%, 68.78%, and 20.98%, respectively. The signals of LAC XPS spectra at 532.10 eV, 530.58 eV, 529.62 eV are attributed to C-OH, -O-, C=O, and their contents are 69.53%, 28.56%, and 1.91%, respectively [44]. By comparison, it could be concluded that the ether bond and C=O on lignin-2 were seriously destroyed in the process of high-temperature activation. Figure 5E,F show the surface morphological features of lignin-1 and LAC, respectively. The surface of lignin-2 was smooth and dense, with few deep pores. However, after carbonization and activation, large amounts of pores appeared on the surface of LAC, which was in line with BET results. A large number of pores would provide more adsorption sites for LAC to purify wastewater containing heavy metal ions.
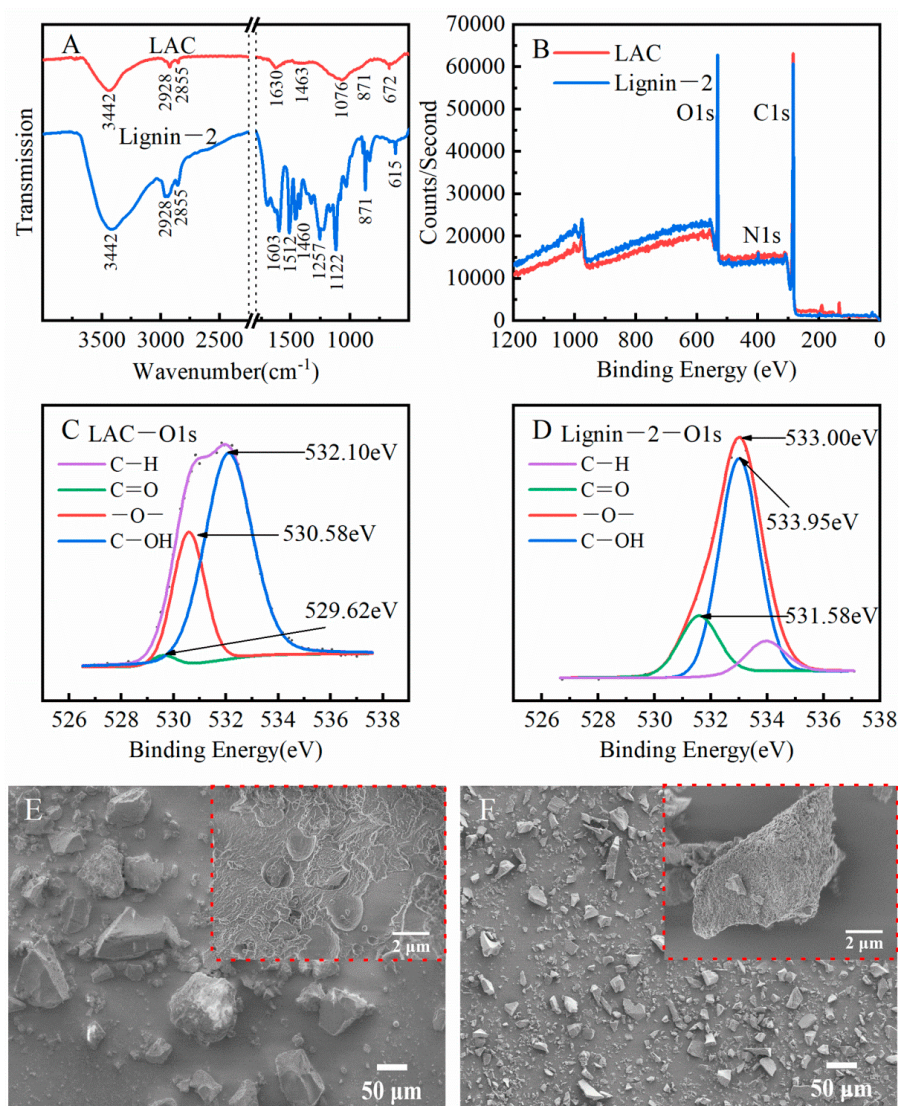

Figure 5. (**A**) FTIR spectra, (**B**–**D**) XPS spectra and (**E**,**F**) SEM of lignin-2 and LAC.

2.6. Adsorption of LAC to Wastewater Containing Cu (II)

2.6.1. Adsorption Isotherms and Adsorption Kinetics

The adsorption isotherm is often used to represent the relationship between the equilibrium concentration and the adsorption capacity, which is helpful for revealing the adsorption mechanism. The Langmuir model [45] and Freundlich model [46] were used to study the equilibrium of copper ions between liquid and solid phases; the detailed analysis process is shown in Text S1. In short, the adsorption process of copper ions by LAC was suitable for the Freundlich model, and the experimental maximum adsorption capacity (79.65 mg/L) was very close to the theoretically calculated maximum adsorption capacity. This result proved that the adsorption process belonged to multi-layer adsorption and heterogeneous adsorption, which was beneficial for improving the adsorption capacity of LAC.

The adsorption kinetics of LAC adsorption of copper ions was studied using two kinetic models derived from pseudo-first-order and pseudo-second-order models [47]; the detailed analysis process is shown in Text S2. The results showed that the R^2 values of the first-order model and the second-order model were both greater than 99%, indicating that the adsorption of copper ions by LAC included both physical adsorption and chemical adsorption. This was a manifestation of the LAC with high adsorption capability.

2.6.2. Effect of LAC Dosage

From Figure 6A, the removal rate of Cu (II) increased gradually as the dosage increased, and the removal rate was over 98% at the LAC dosage of 0.8 g/L. Adsorption sites increased with larger dosage of LAC. Even if the concentration of Cu (II) in wastewater was quite low, enough adsorption sites could still effectively adsorb Cu (II). However, the adsorption capacity of LAC decreased gradually with increasing LAC dosage. When the dosage of LAC increased, Cu (II) was more easily adsorbed on the surface of LAC and many adsorption sites were not utilized, resulting in a lower adsorption capacity.
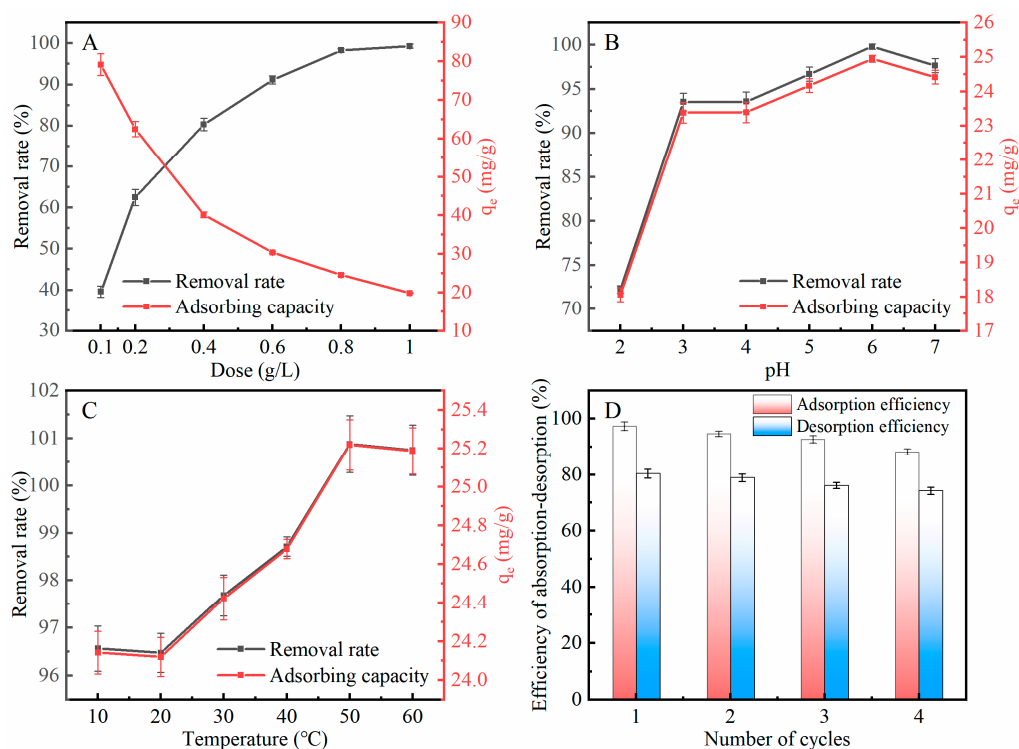

Figure 6. Effects of (**A**) dose, (**B**) wastewater pH, (**C**) temperature and (**D**) number of cycles on the removal rate and the adsorption capacity. Error bars represent the standard deviation from three repetitions.

2.6.3. Effect of Wastewater pH

The applicability of adsorbents to wastewater with different pH was an important factor to evaluate the quality of adsorbents [48]. The effect of pH on the adsorption performance of LAC is shown in Figure 6B. At increasing pH (from 2.0 to 3.0), the removal rate and adsorption capacity of LAC showed an upward trend. At the pH range 3.0–6.0, the removal rate and adsorption capacity of LAC gradually increased with the increase of wastewater pH. In a strong acid environment (pH = 2), the negatively charged functional groups on LAC were difficult to ionize, and a large number of hydrogen ions increased the electrostatic repulsion between LAC and copper ions, resulting in poor adsorption effect. With the increase of pH, the electrostatic repulsion between LAC and copper ions was weakened due to the reduction of hydrogen ions, and the adsorption effect was enhanced under the action of electrostatic attraction and chelation [49]. When the wastewater pH value was 6, the removal rate of copper ions by LAC was nearly 100%. However, as the wastewater pH value continued to increase, the adsorption effect of LAC decreased. This was because when the pH value was higher than 6, copper ions started to precipitate, which limited the adsorption effect of LAC. In general, LAC exhibited high adsorption capacity for copper ions over a wide pH range, except for strong acid environments.

2.6.4. Effect of Temperature

The Brownian motion of copper ions and their diffusion on LAC surface and pore of were affected by temperature. Figure 6C shows that LAC had excellent adsorption effect on copper ions at all temperatures (10~60 °C). The adsorption effect increased at increasing temperature, proving that the process was endothermic. Moreover, higher temperature could increase the number of activated molecules on LAC and increase the contact probability between LAC and copper ions, improving the adsorption effect. However, the adsorption capacity of LAC decreased slightly when the temperature was higher than 50 °C. This was attributed to the excessively high temperature intensifying Brownian motion, which made the heavy metal ions on the adsorbent surface overactive. Some heavy metal ions were desorbed immediately before entering the adsorbent, thus inhibiting the progress of adsorption.

2.6.5. Regeneration of LAC

The reproducibility and reusability of LAC are important parameters to measure its commercialization potential. In this study, the reproducibility and reusability of LAC were tested by four consecutive adsorption–desorption cycles, and the detailed procedures were described in Text S3. From Figure 6D, the cyclic investigation showed that adsorption efficiencies of LAC were 97.32%, 94.63%, 92.63%, and 88.12% from the four cycles, respectively, while the desorption efficiencies were 80.40%, 78.92%, 76.15%, and 74.26%, respectively. It could be found that both the adsorption and desorption efficiencies of LAC decreased after cycling, which was attributed to the hard-to-desorb copper ions and the aging of a small part of the adsorption sites [50]. Satisfyingly, after four cycles, LAC still had 88.12% adsorption efficiency and 74.26% desorption efficiency, indicating the outstanding reusability of LAC.

2.6.6. Prospect of Industrialization

The technology proposed in this study has great prospects for large-scale production due to its advantages of easy operation, cost-effectiveness, and low pollution. Considering the industrialization cost of lignin fractionation, one-step ethanol fractionation of industrial lignin can achieve similar effects as above, reducing the difficulty and cost of fractionation. Moreover, the synthetic process of lignin-based flocculants in this paper avoided the use of a number of expensive, harmful solvents, such as dioxane, high-concentration alkaline solutions, etc., which is cost- and eco-efficient. It is worth noting that the recovery and reuse of ethanol from either fractionation processes or the preparation of lignin-based flocculants can be easily achieved in industrialization. Regarding the preparation process

of lignin-based activated carbon, the carbonization process and the activation process are integrated, which simplifies the steps and reduces the cost. In particular, combining the technology in this study with the corn cob biorefinery process (production of xylose, ethanol) can greatly improve the utilization rate of biomass, characterized by environmental friendliness, cost-effectiveness, and ecological benefits.

3. Materials and Methods

3.1. Materials

The alkali lignin (KL) isolated from corn cob was supplied by Shandong Longlive Biotechnology Co., Ltd. (Dezhou, China). In short, corn cob was first subjected to hydrothermal treatment in order to degrade hemicellulose, and then the residue was treated with an alkaline solution (1.5% NaOH) for 3 h at 80 °C. Finally, the KL was obtained by adjusting the lignin-rich alkaline solution to acidity. N-butanol, ethanol, methanol, dioxane, trimethyl-2-methacroyloxyethylammonium chloride (METAC), azobisisobutyronitrile (AIBN), kaolin, and H_3PO_4 were purchased from Sinopharm Group Co., Ltd. (Beijing, China).

3.2. Sequential Solvent Fractionation

As shown in Scheme 2, industrial alkali lignin (KL) from corn cob was fractionated sequentially using five recoverable organic solvents. The specific procedure in detail has been explained in our previous studies [23]. Finally, the lignin fractions collected from n-butanol, ethanol, methanol, and dioxane were referred as F1, F2, F3, and F4, respectively, and F5 was an insoluble residue.
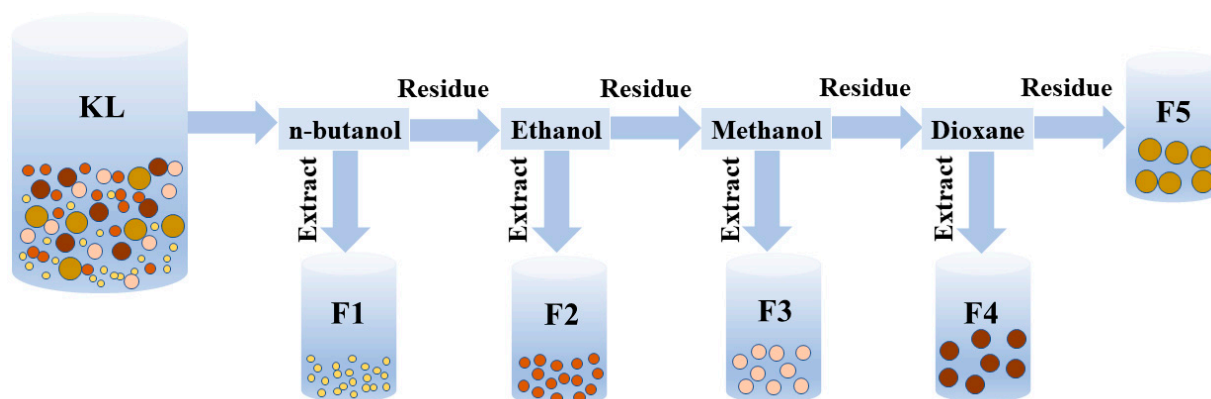
Scheme 2. Scheme for organic solvent fractionation of KL.

3.3. Production of a Lignin-Based Flocculant

Based on full structural interpretation of all lignin, lignin-based flocculants were produced in ethanol solvent using lignin with high reactivity and accessibility as raw material, METAC as monomer, and AIBN as initiator. A certain proportion of lignin, METAC, and AIBN were added to the reactor. The reaction temperatures were 50, 60, 70 and 80 °C, respectively, for different times (2, 3, 4, and 5 h) under N_2 condition. At complete reaction, the mixture was added dropwise to 3 volumes of acetone to collect the precipitate. The precipitate was then washed with acetone several times, and the pure lignin-based flocculant was gained after lyophilization. Referring to the aforementioned steps, PMETAC was produced by the conditions of 0.42 g AIBN, 14 g METAC, 4 h, and 60 °C.

3.4. Production of Lignin-Based Activated Carbon

The lignin consisting of high content of carbon was mixed with 85% phosphoric acid according to different impregnation ratios (phosphoric acid:F4 was 0.5:1~2.5:1), and nitrogen (500 mL/min) was used as protective gas for carbonization activation in a tubular furnace at 800 °C for 90 min. The obtained carbonized products were further purified by washing with hydrochloric acid, and followed by deionized water to adjust pH to

7.0. Finally, the carbonized products washed to neutral were dried at 105 °C to obtain lignin-based activated carbon.

3.5. Characterization

FT-IR of all samples was analyzed via a Brock tensor II spectrometer by the KBr pellet method; 2D-HSQC and ^{31}P NMR were determined by a Bruker AVIII [51,52]. The determination methods of zeta potential and molecular weight of samples were described in previous studies [38,53]. The SEM micrographs were obtained by magnifying samples 200 and 10,000 times under 1.0 kV acceleration voltage using an emission scanning electron microscope (SU8020, Hitachi, Tokyo, Japan) [54]. XPS spectra of LAC and lignin-2 were recorded by the XASAM 800 spectrometer (Kratos Analytical, Manchester, UK) to analyze the content of elements in LAC and lignin-2 [44]. The specific surface analysis (BET) was determined by an ASAP 2020M (Micromeritics, Norcross, GA, USA) after degassing the dried samples at 200 °C for 7 h [55,56].

3.6. Flocculation Experiments

Flocculation experiments were performed using kaolin suspensions as simulated wastewater. Lignin-based flocculant was added into 100 mL kaolin suspension. After that, a mechanical stirring device was used to stir for 3 min (250 rpm), followed by 15 min (100 rpm), and finally the mixture stood for 90 min. The turbidity of kaolin suspension before and after flocculation was measured by WGZ-200S (Shanghai Xinrui Instrument Co., Ltd.), expressed by (T_0) and (T_t), respectively. The removal rate was calculated by the following formula:

$$\text{Removal rate} = (T_0 - T_t)/\ T_0 \times 100\% \tag{1}$$

3.7. Adsorption Experiments

To a solution of Cu (II) solution (25 mL, 20 mg/L, pH = 5.8), LAC was added and then stirred for 120 min. After that, the supernatant was collected via a 0.45 μm membrane. Then the filtrate was measured by ICP (SPECTROBLUE ICP-OES, Spike Analytical Instruments, Germany) to determine the remaining Cu (II) content. The Cu (II) removal rate and the LAC adsorption capacity (q_e) were calculated by the following formula:

$$\text{removal rate} = (C_0 - C_t)/C_0 \times 100\% \tag{2}$$

$$q_e = (C_0 - C_t) \times V/D \tag{3}$$

where C_0 and C_t (mg/L) stand for the concentrations of Cu (II) before and after adsorption, respectively. V (mL) represented the solution volume of added Cu (II), and D (mg) indicated the dosage of LAC.

4. Conclusions

In order to produce lignin-based products more cleanly, industrial lignin was divided into several more homogeneous lignin fractions by organic solvent fractionation, and the structure of each fraction was adequately deciphered. Lignin-1 fractionated from ethyl acetate and ethanol had superior reactivity and reaction accessibility, and was used as raw material to produce lignin-based flocculant in green, inexpensive and recyclable ethanol solvents. Lignin-2 fractionated from methanol and dioxane had a high carbon content and was used as a precursor for the production of activated carbon. After optimizing the reaction conditions, LBF with removal rate of over 98% for kaolin suspension and LAC with 79.65 mg/g adsorption capacity for copper ion were successfully produced. The flocculation mechanism of LBF-treated kaolin suspension was charge attraction and bridging, and the adsorption of copper ions by LAC belonged to the multi-layer adsorption under the combined action of physical adsorption and chemical adsorption. Moreover, both LBF and LAC could be well applied to wastewater with complex external environment, showing great commercialization potential. The strategy of obtaining the desired lignin

components by lignin fractionation and then making targeted high-value utilization of them is expected to be applied to the preparation of other lignin-based products. In addition, strengthening the structural interpretation of lignin and its derivatives, and establishing a stable structure–activity relationship are inevitable ways to develop lignin-based products in the future.

References

1. Sakudo, A.; Yagyu, Y.; Onodera, T. Disinfection and sterilization using plasma technology: Fundamentals and future perspectives for biological applications. *Int. J. Mol. Sci.* **2019**, *20*, 5216. [CrossRef] [PubMed]
2. Teh, C.Y.; Budiman, P.M.; Shak, K.P.Y.; Wu, T.Y. Recent advancement of coagulation–flocculation and its application in wastewater treatment. *Ind. Eng. Chem. Res.* **2016**, *55*, 4363–4389. [CrossRef]
3. Wang, B.; Wang, S.F.; Lam, S.S.; Sonne, C.; Yuan, T.Q.; Song, G.Y.; Sun, R.C. A review on production of lignin-based flocculants: Sustainable feedstock and low carbon footprint applications. *Renew. Sustain. Energy Rev.* **2020**, *134*, 110384. [CrossRef]
4. Kumar, A.; Biswas, B.; Kaur, R.; Krishna, B.B.; Bhaskar, T. Hydrothermal oxidative valorisation of lignin into functional chemicals: A review. *Bioresour. Technol.* **2021**, *342*, 126016. [CrossRef] [PubMed]
5. Wang, B.; Sun, D.; Yuan, T.; Song, G.; Sun, R. Recent Advances in Lignin Modification and Its Application in Wastewater Treatment. *Lignin Util. Strateg. Processing Appl.* **2021**, *1377*, 143–173.
6. Vanholme, R.; Demedts, B.; Morreel, K.; Ralph, J.; Boerjan, W. Lignin biosynthesis and structure. *Plant Physiol.* **2010**, *153*, 895–905. [CrossRef]
7. Beisl, S.; Friedl, A.; Miltner, A. Lignin from micro-to nanosize: Applications. *Int. J. Mol. Sci.* **2017**, *18*, 2367. [CrossRef]
8. Xu, R.; Du, H.S.; Liu, C.; Liu, H.Y.; Wu, M.Y.; Zhang, X.Y.; Si, C.L.; Li, B. An efficient and magnetic adsorbent prepared in a dry process with enzymatic hydrolysis residues for wastewater treatment. *J. Clean. Prod.* **2021**, *313*, 127834. [CrossRef]
9. Yuan, H.; Peng, J.; Ren, T.; Luo, Q.; Luo, Y.; Zhang, N.; Huang, Y.; Guo, X.; Wu, Y. Novel fluorescent lignin-based hydrogel with cellulose nanofibers and carbon dots for highly efficient adsorption and detection of Cr (VI). *Sci. Total Environ.* **2021**, *760*, 143395. [CrossRef]
10. Kwak, H.W.; Shin, M.; Yun, H.; Lee, K.H. Preparation of silk sericin/lignin blend beads for the removal of hexavalent chromium ions. *Int. J. Mol. Sci.* **2016**, *17*, 1466. [CrossRef]
11. Brodin, M.; Vallejos, M.; Opedal, M.T.; Area, M.C.; Chinga-Carrasco, G. Lignocellulosics as sustainable resources for production of bioplastics—A review. *J. Clean. Prod.* **2017**, *162*, 646–664. [CrossRef]
12. Gioia, C.; Colonna, M.; Tagami, A.; Medina, L.; Sevastyanova, O.; Berglund, L.A.; Lawoko, M. Lignin-based epoxy resins: Unravelling the relationship between structure and material properties. *Biomacromolecules* **2020**, *21*, 1920–1928. [CrossRef] [PubMed]
13. Baumberger, S.P.; Lapierre, C.; Monties, B. Utilization of pine kraft lignin in starch composites: Impact of structural heterogeneity. *J. Agric. Food Chem.* **1998**, *46*, 2234–2240. [CrossRef]
14. Wang, Q.; Guo, J.; Lu, X.; Ma, X.; Cao, S.; Pan, X.; Ni, Y. Wearable lignin-based hydrogel electronics: A mini-review. *Int. J. Biol. Macromol.* **2021**, *181*, 45–50. [CrossRef] [PubMed]
15. Gigli, M.; Crestini, C. Fractionation of industrial lignins: Opportunities and challenges. *Green Chem.* **2020**, *22*, 4722–4746. [CrossRef]
16. Fernández-Rodríguez, J.; Erdocia, X.; Hernández-Ramos, F.; Alriols, M.G.; Labidi, J. Lignin separation and fractionation by ultrafiltration. In *Separation of Functional Molecules in Food by Membrane Technology*; Charis, M., Galanakis, C.M., Eds.; Academic Press: London, UK, 2019; pp. 229–265.

17. Araújo, L.C.P.; Yamaji, F.M.; Lima, V.H.; Botaro, V.R. Kraft lignin fractionation by organic solvents: Correlation between molar mass and higher heating value. *Bioresour. Technol.* **2020**, *314*, 123757. [CrossRef]

18. Passoni, V.; Scarica, C.; Levi, M.; Turri, S.; Griffini, G. Fractionation of industrial softwood kraft lignin: Solvent selection as a tool for tailored material properties. *ACS Sustain. Chem. Eng.* **2016**, *4*, 2232–2242. [CrossRef]

19. Schuerch, C. The solvent properties of liquids and their relation to the solubility, swelling, isolation and fractionation of lignin. *J. Am. Chem. Soc.* **1952**, *74*, 5061–5067. [CrossRef]

20. Kim, J.Y.; Park, S.Y.; Lee, J.H.; Choi, I.G.; Choi, J.W. Sequential solvent fractionation of lignin for selective production of monoaromatics by Ru catalyzed ethanolysis. *RSC Adv.* **2017**, *7*, 53117–53125. [CrossRef]

21. Duarah, P.; Haldar, D.; Purkait, M.K. Technological advancement in the synthesis and applications of lignin-based nanoparticles derived from agro-industrial waste residues: A review. *Int. J. Biol. Macromol.* **2020**, *163*, 1828–1843. [CrossRef]

22. Figueiredo, P.; Lintinen, K.; Hirvonen, J.T.; Kostiainen, M.A.; Santos, H.A. Properties and chemical modifications of lignin: Towards lignin-based nanomaterials for biomedical applications. *Prog. Mater. Sci.* **2018**, *93*, 233–269. [CrossRef]

23. Liu, Z.C.; Wang, Z.W.; Gao, S.; Tong, Y.X.; Le, X.; Hu, N.W.; Yan, Q.S.; Zhou, X.G.; He, Y.R.; Wang, L. Isolation and Fractionation of the Tobacco Stalk Lignin for Customized Value-Added Utilization. *Front. Bioeng. Biotechnol.* **2021**, *9*, 811287. [CrossRef] [PubMed]

24. Ling, J.K.U.; Hadinoto, K. Deep Eutectic Solvent as Green Solvent in Extraction of Biological Macromolecules: A Review. *Int. J. Mol. Sci.* **2022**, *23*, 3381. [CrossRef] [PubMed]

25. Huang, C.; Lin, W.; Lai, C.; Li, X.; Jin, Y.; Yong, Q. Coupling the post-extraction process to remove residual lignin and alter the recalcitrant structures for improving the enzymatic digestibility of acid-pretreated bamboo residues. *Bioresour. Technol.* **2019**, *285*, 121355. [CrossRef] [PubMed]

26. Faix, O. Classification of lignins from different botanical origins by FT-IR spectroscopy. *Holzforschung* **1991**, *45*, 21–28. [CrossRef]

27. Wang, B.; Sun, D.; Wang, H.M.; Yuan, T.Q.; Sun, R.C. Green and facile preparation of regular lignin nanoparticles with high yield and their natural broad-spectrum sunscreens. *ACS Sustain. Chem. Eng.* **2018**, *7*, 2658–2666. [CrossRef]

28. Yuan, T.Q.; Sun, S.N.; Xu, F.; Sun, R.C. Characterization of lignin structures and lignin-carbohydrate complex (LCC) linkages by quantitative 13C and 2D HSQC NMR spectroscopy. *J. Agric. Food Chem.* **2011**, *59*, 10604–10614. [CrossRef]

29. Heikkinen, S.; Toikka, M.M.; Karhunen, P.T.; Kilpeläinen, I.A. Quantitative 2D HSQC (Q-HSQC) via suppression of J-dependence of polarization transfer in NMR spectroscopy: Application to wood lignin. *J. Am. Chem. Soc.* **2003**, *125*, 4362–4367. [CrossRef]

30. Sette, M.; Wechselberger, R.; Crestini, C. Elucidation of lignin structure by quantitative 2D NMR. *Chem.-A Eur. J.* **2011**, *17*, 9529–9535. [CrossRef]

31. Ikeda, T.; Holtman, K.; Kadla, J.F.; Chang, H.M.; Jameel, H. Studies on the effect of ball milling on lignin structure using a modified DFRC method. *J. Agric. Food Chem.* **2002**, *50*, 129–135. [CrossRef]

32. Wang, B.; Wang, H.M.; Sun, D.; Yuan, T.Q.; Song, G.Y.; Shi, Q.; Zheng, L.; Wang, S.F.; Sun, R.C. Chemosynthesis, characterization and application of lignin-based flocculants with tunable performance prepared by short-wavelength ultraviolet initiation. *Ind. Crops Prod.* **2020**, *157*, 112897. [CrossRef]

33. Chen, R.; Kokta, B.; Valade, J. Study on the graft copolymerization of lignosulfonate and acrylic monomers. *J. Appl. Polym. Sci.* **1980**, *25*, 2211–2220. [CrossRef]

34. Wang, B.; Sun, Z.; Lam, S.S.; Sonne, C.; Yuan, T.Q.; Sun, R.C. A scalable and simple lignin-based polymer for ultra-efficient flocculation and sterilization. *Sep. Purif. Technol.* **2022**, *292*, 120960. [CrossRef]

35. Georges, M.K.; Veregin, R.P.; Kazmaier, P.M.; Hamer, G.K. Narrow molecular weight resins by a free-radical polymerization process. *Macromolecules* **1993**, *26*, 2987–2988. [CrossRef]

36. Binyuan, Z.; Keao, H.; Yongzhong, F.; Rinfang, Z.; Renjie, W. Infrared spectroscopic study on lignosulfonic acid and its derivatives. *Chin. J. Anal. Chem.* **2000**, *120*. [CrossRef]

37. Fang, R.; Cheng, X.; Xu, X. Synthesis of lignin-base cationic flocculant and its application in removing anionic azo-dyes from simulated wastewater. *Bioresour. Technol.* **2010**, *101*, 7323–7329. [CrossRef]

38. Salopek, B.; Krasic, D.; Filipovic, S. Measurement and application of zeta-potential. *Rud.-Geol.-Naft. Zb.* **1992**, *4*, 147.

39. Dickinson, E.; Eriksson, L. Particle flocculation by adsorbing polymers. *Adv. Colloid Interface Sci.* **1991**, *34*, 1–29. [CrossRef]

40. Zhao, X.; Wang, X.; Song, G.; Lou, T. Microwave assisted copolymerization of sodium alginate and dimethyl diallyl ammonium chloride as flocculant for dye removal. *Int. J. Biol. Macromol.* **2020**, *156*, 585–590. [CrossRef]

41. Jia, S.; Yang, Z.; Ren, K.; Tian, Z.; Dong, C.; Ma, R.; Yu, G.; Yang, W. Removal of antibiotics from water in the coexistence of suspended particles and natural organic matters using amino-acid-modified-chitosan flocculants: A combined experimental and theoretical study. *J. Hazard. Mater.* **2016**, *317*, 593–601. [CrossRef]

42. Yu, X.; Somasundaran, P. Role of polymer conformation in interparticle-bridging dominated flocculation. *J. Colloid Interface Sci.* **1996**, *177*, 283–287. [CrossRef]

43. Li, K.; Li, P.; Cai, J.; Xiao, S.; Yang, H.; Li, A. Efficient adsorption of both methyl orange and chromium from their aqueous mixtures using a quaternary ammonium salt modified chitosan magnetic composite adsorbent. *Chemosphere* **2016**, *154*, 310–318. [CrossRef] [PubMed]

44. Babeła, K.; Jurewicz, K. KOH activated lignin based nanostructured carbon exhibiting high hydrogen electrosorption. *Carbon* **2008**, *46*, 1948–1956. [CrossRef]

45. Langmuir, I. The adsorption of gases on plane surfaces of glass, mica and platinum. *J. Am. Chem. Soc.* **1918**, *40*, 1361–1403. [CrossRef]

46. Freundlich, H. Over the adsorption in solution. *J. Phys. Chem* **1906**, *57*, 1100–1107.

47. Lagergren, S. Zur theorie der sogenannten adsorption geloster stoffe. *K. Sven. Vetensk. Handl.* **1898**, *24*, 1–39.

48. Salam, O.E.A.; Reiad, N.A.; ElShafei, M.M. A study of the removal characteristics of heavy metals from wastewater by low-cost adsorbents. *J. Adv. Res.* **2011**, *2*, 297–303. [CrossRef]

49. Elliott, H.; Huang, C. The adsorption characteristics of Cu (II) in the presence of chelating agents. *J. Colloid Interface Sci.* **1979**, *70*, 29–45. [CrossRef]

50. Dickey, F.H. Specific adsorption. *J. Phys. Chem.* **1955**, *59*, 695–707. [CrossRef]

51. Río, J.C.D.; Rencoret, J.; Prinsen, P.; Martínez, Á.T.; Ralph, J.; Gutiérrez, A. Structural characterization of wheat straw lignin as revealed by analytical pyrolysis, 2D-NMR, and reductive cleavage methods. *J. Agric. Food Chem.* **2012**, *60*, 5922–5935.

52. Wen, J.L.; Sun, S.L.; Yuan, T.Q.; Xu, F.; Sun, R.C. Structural elucidation of lignin polymers of Eucalyptus chips during organosolv pretreatment and extended delignification. *J. Agric. Food Chem.* **2013**, *61*, 11067–11075. [CrossRef] [PubMed]

53. Tolbert, A.; Akinosho, H.; Khunsupat, R.; Naskar, A.K.; Ragauskas, A.J. Characterization and analysis of the molecular weight of lignin for biorefining studies. *Biofuels Bioprod. Biorefining* **2014**, *88*, 836–856. [CrossRef]

54. Fu, K.; Yue, Q.; Gao, B.; Sun, Y.; Zhu, L. Preparation, characterization and application of lignin-based activated carbon from black liquor lignin by steam activation. *Chem. Eng. J.* **2013**, *228*, 1074–1082. [CrossRef]

55. Li, Z.; Chen, J.; Ge, Y. Removal of lead ion and oil droplet from aqueous solution by lignin-grafted carbon nanotubes. *Chem. Eng. J.* **2017**, *308*, 809–817. [CrossRef]

56. Li, Z.; Xiao, D.; Ge, Y.; Koehler, S. Surface-functionalized porous lignin for fast and efficient lead removal from aqueous solution. *ACS Appl. Mater. Interfaces* **2015**, *7*, 15000–15009. [CrossRef]

57. Wang, Y.; Wang, H.; Peng, H.; Wang, Z.; Wu, J.; Liu, Z. Dye adsorption from aqueous solution by cellulose/chitosan composite: Equilibrium, kinetics, and thermodynamics. *Fibers Polym.* **2018**, *19*, 340–349. [CrossRef]

58. Lakey, P.S.; Eichler, C.M.; Wang, C.; Little, J.C.; Shiraiwa, M. Kinetic multi-layer model of film formation, growth, and chemistry (KM-FILM): Boundary layer processes, multi-layer adsorption, bulk diffusion, and heterogeneous reactions. *Indoor Air* **2021**, *31*, 2070–2083. [CrossRef]

59. Al-Ghouti, M.A.; Da'ana, D.A. Guidelines for the use and interpretation of adsorption isotherm models: A review. *J. Hazard. Mater.* **2020**, *393*, 122383. [CrossRef]

60. Wang, X.; Li, X.; Peng, L.; Han, S.; Hao, C.; Jiang, C.; Wang, H.; Fan, X. Effective removal of heavy metals from water using porous lignin-based adsorbents. *Chemosphere* **2021**, *279*, 130504. [CrossRef]